

# Role of $\alpha$ -SNAP in Promoting Efficient Neurotransmission at the Crayfish Neuromuscular Junction

PING HE,<sup>1</sup> R. CHASE SOUTHARD,<sup>1</sup> DONG CHEN,<sup>2</sup> S. W. WHITEHEART,<sup>2</sup> AND R. L. COOPER<sup>1</sup>

<sup>1</sup>*T. H. Morgan School of Biological Science, University of Kentucky, Lexington 40506-0225; and* <sup>2</sup>*Department of Biochemistry, University of Kentucky College of Medicine, Lexington, Kentucky 40536-0084*

**He, Ping, R. Chase Southard, Dong Chen, S. W. Whiteheart, and R. L. Cooper.** Role of  $\alpha$ -SNAP in promoting efficient neurotransmission at the crayfish neuromuscular junction. *J. Neurophysiol.* 82: 3406–3416, 1999. In this manuscript, we address the role of the soluble N-ethylmaleimide sensitive factor attachment protein ( $\alpha$ -SNAP) in synaptic transmission at the neuromuscular junction of the crayfish opener muscle. Immunohistochemical methods confirm the presence of  $\alpha$ -SNAP in these preparations and show that it is concentrated in the synaptic areas. Microinjection and electrophysiological studies show that  $\alpha$ -SNAP causes an increase in neurotransmitter release yet does not significantly affect the kinetics. More specific quantal analysis, using focal, macropatch, synaptic current recordings, shows that  $\alpha$ -SNAP increases transmitter release by increasing the probability of exocytosis but not the number of potential release sites. These data demonstrate that the role of  $\alpha$ -SNAP is to increase the efficiency of neurotransmission by increasing the probability that a stimulus will result in neurotransmitter release. What this suggests is that  $\alpha$ -SNAP is critical for the formation and maintenance of a “ready release” pool of synaptic vesicles.

## INTRODUCTION

The studies of neurotransmitter (NT) release have yielded a long list of molecules, proposed to play a role in neurotransmission and have suggested an outline of a molecular interactions required for synaptic vesicle (SV) exocytosis (reviewed in Bajjalieh and Scheller 1995; Martin 1997; Rothman 1994; Sudhof 1995). Membrane proteins from the synaptic vesicle [called vesicle soluble N-ethylmaleimide sensitive factor attachment protein receptors (v-SNAREs), e.g., vesicle associated membrane protein (VAMP)/synaptobrevin] and from the active zone [called target membrane SNAREs (t-SNAREs), e.g., syntaxin and synaptosome associated protein 23 or 25 (SNAP23/25)] appear to be essential for membrane fusion events (Hunt et al. 1994; Littleton et al. 1998; Weber et al. 1998). Current data suggest that the three SNARE proteins, interlocked by the interactions of their coiled-coil domains (Poirier et al. 1998; Sutton et al. 1998; Weber et al. 1998), form a bimembrane-spanning complex that is sufficient for bilayer fusion (Weber et al. 1998).

The interactions of the SNARE proteins are, in part, regulated by cytosolic proteins called SNAPs and NSF (N-ethylmaleimide sensitive factor). SNAPs initially bind to the SNARE complex and serve as adapters to correctly position NSF (Clary et al. 1990; Weidman et al. 1989). SNAP is also

responsible for the stimulation of NSF's ATPase activity, which in turn is needed to disassemble the SNARE complex (Barnard et al. 1997; Nagiec et al. 1995). Although SNAREs are needed for fusion (Hunt et al. 1994; Littleton et al. 1998; Weber et al. 1998), it is less obvious what role SNAP and NSF play in neurotransmission (Banerjee et al. 1996; Haas and Wickner 1996; Hay and Martin 1992; Martin et al. 1995; Mayer and Wickner 1997; Mayer et al. 1996). Injection studies using squid axons have shown that SNAPs increase the output of a terminal (DeBello et al. 1995). Similar studies have shown that NSF increases the efficiency of NT release (Schweizer et al. 1998). Studies with the comatose mutant in *Drosophila* (temperature-sensitive NSF) have demonstrated that active NSF is required for SV consumption and have suggested that NSF functions both before and after membrane fusion (Kawasaki et al. 1998; Littleton et al. 1998; Siddiqi and Benzer 1976; Tolar and Pallanck 1998). The model emerging from this research suggests that NSF and SNAPs are involved in both SNARE priming before fusion and in SNARE recycling after membrane fusion.

In this study, we used the opener neuromuscular junction (NMJ) from the crayfish to assess the role of  $\alpha$ -SNAP on NT release. In microinjection studies,  $\alpha$ -SNAP increased synaptic output with only a small effect on release kinetics. Quantal analysis indicates that  $\alpha$ -SNAP had no effect on the total number of release sites but significantly increased the probability that a stimulus will result in NT release. Consistently,  $\alpha$ -SNAP injection reduced the failure rate for evoked NT release. These data indicate that  $\alpha$ -SNAP is not involved in the membrane fusion event but, like NSF (Schweizer et al. 1998), functions to increase the pool of “ready release” SVs at the synapse. Preliminary reports of this study have appeared in abstract form (He et al. 1997; Southard et al. 1998).

This work is in partial fulfillment of the Master of Science degree requirement for P. He.

## METHODS

### *Western blotting analysis of crayfish tissues*

Crayfish tissue, consisting of the ventral nerve cord and the identified abdominal extensor muscle (containing motor nerve terminals) were dissected and then homogenized using a Dounce homogenizer in lysis buffer [(in mM) 25 Tris/HCl (pH 8.0), 500 KCl, 250 sucrose, 2 EGTA, and 0.5 1,10-phenanthroline] with 1% (vol/vol) Triton X-100. After incubation on ice for 45 min., the insoluble material was removed by centrifugation. The protein concentrations of the detergent-solubilized proteins were measured using the bicinchoninic acid assay (Pierce, Rockford, IL) with bovine serum albumin (Sigma, St.

The costs of publication of this article were defrayed in part by the payment of page charges. The article must therefore be hereby marked “advertisement” in accordance with 18 U.S.C. Section 1734 solely to indicate this fact.

Louis, MO) as standard. For Western blotting analysis, 150  $\mu$ g of crayfish extract was fractionated by 10% SDS-PAGE and transferred to nitrocellulose. Blots then were probed with anti- $\alpha$ -SNAP antibodies (Whiteheart et al. 1992), and the immunodecorated proteins were detected by Enhanced Chemiluminescence (ECL, Pierce) using anti-rabbit IgG secondary antibodies conjugated to horseradish peroxidase (Sigma). Similarly prepared, rat brain extracts were used as positive blotting controls.

### Immunofluorescence

Whole-mount preparations were pinned to a silicone elastomer (Sylgard) dish with the muscle in a stretched position. They were fixed with 2.5% (vol/vol) glutaraldehyde, 0.5% (vol/vol) formaldehyde dissolved in a buffer A (0.1 M sodium cacodylate, pH 7.4, 0.022% wt  $\text{CaCl}_2$ , 4% wt sucrose) for 1 h with two changes of solution. The preparation then was placed into vials and washed in buffer A containing 0.2% (vol/vol) TritonX-100 and 1% (vol/vol) normal goat serum (Gibco/BRL, Grand Island, NY) for 1 h with three changes at room temperature. The tissue then was incubated with primary antibody to  $\alpha$ -SNAP [1:1000 in PBS buffer (in mM): 136 NaCl, 2.7 KCl, 10  $\text{Na}_2\text{HPO}_4$ , and 1.5 mM  $\text{KH}_2\text{PO}_4$ ] in a shaker at 4°C for 12 h. The tissue was washed three times and incubated in secondary antibody (goat, anti-rabbit IgG conjugated with Texas Red, Sigma) diluted 1:200 with PBS buffer at room temperature for 2 h, followed by two washes in buffer. The synaptic locations were observed by immunocytochemistry as previously shown in nerve terminals (Cooper 1998; Cooper et al. 1996a). Fluorescent images of the nerve terminals (Fig. 1, A and B) were obtained with a Nikon Optiphot-2 upright fluorescent microscope using a  $\times 40$  (0.55 NA) Nikon water immersion objective (Nikon, Melville, NY) with appropriate illumination.

### Preparation of $\alpha$ -SNAP and $\alpha$ -SNAP(L294A) mutant

The  $\alpha$ -SNAP(L294A) mutant (Barnard et al. 1997) expression construct was prepared by PCR, and the point mutation was confirmed by dideoxy sequencing. Recombinant  $\alpha$ -SNAP and the (L294A) mutant were expressed in *Escherichia coli* using the pQE-9 expression vector (Qiagen, Valencia, CA) and purified by  $\text{Ni}^{2+}$  nitrilotriacetic acid agarose affinity chromatography as described in Whiteheart et al. (1993). Both SNAP proteins were dialyzed exhaustively against injection buffer [containing (in mM) 10 HEPES/NaOH (pH 7.4), 115 KAc, 2 glutathione, 3.5  $\text{MgAc}_2$  and 0.5 ATP and 1% (vol/vol) glycerol] and stored at  $-80^\circ\text{C}$  at a concentration of 0.51 mg/ml.

### Crayfish NMJ preparation

All experiments were performed using the first walking leg of crayfish, *Procambarus clarkii* (4–6 cm in body length, Atchafalaya Biological Supply, Raceland, LA). The opener muscle of the first walking legs was prepared by the standard dissection (Cooper and Ruffner 1998; Dudel and Kuffler 1961). The tissue was pinned out in a Sylgard dish for viewing with an Optiphot-2 upright fluorescent microscope using a  $\times 40$  (0.55 NA) water-immersion objective (Nikon). Dissected preparations were maintained in crayfish saline [modified Van Harrevel'd's solution (in mM): 205 NaCl, 5.3 KCl, 13.5  $\text{CaCl}_2$ , 2.45  $\text{MgCl}_2$ , and 0.5 HEPES/NaOH, pH 7.4] at 14°C. The entire opener muscle is innervated by a single tonic excitatory and inhibitory motor neuron (Cooper et al. 1995a). To visualize the nerve terminals, living preparations were stained fluorescently for 2–5 min. with 2–5  $\mu\text{M}$  4-[4-(diethylamino) styryl]-N-methylpyridinium iodide (4-Di-2-Asp; Molecular Probes, Eugene, OR) in crayfish saline.

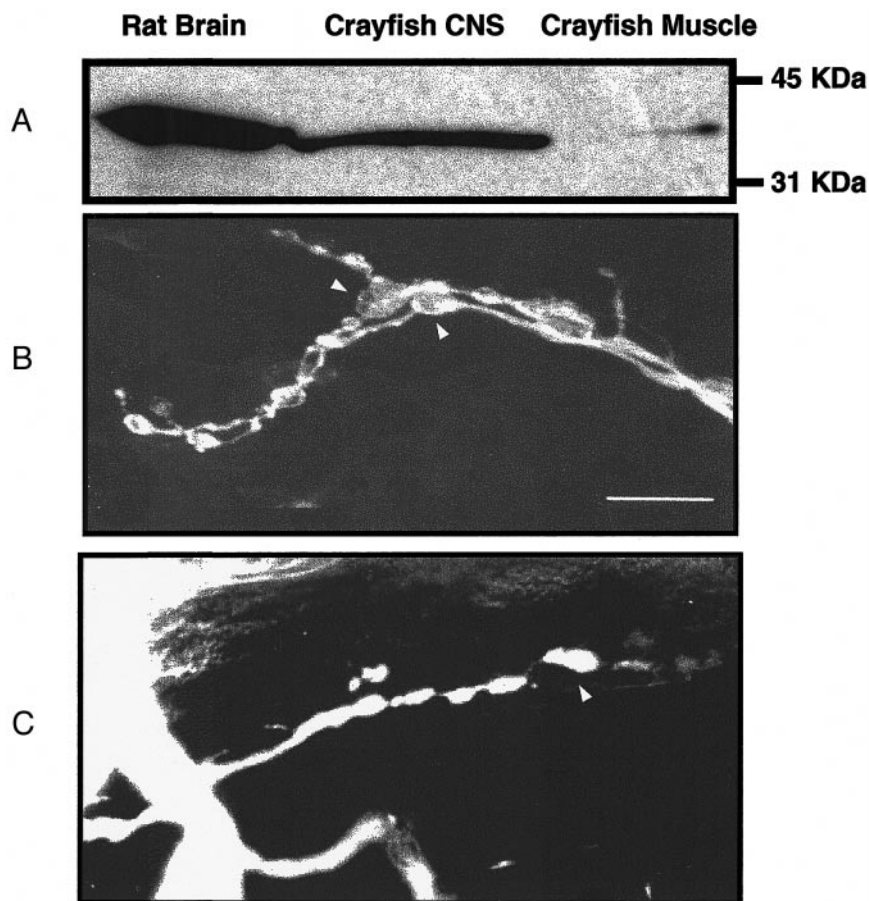


FIG. 1. Identification of  $\alpha$ -soluble *N*-ethylmaleimide-sensitive factor (NSF) attachment protein ( $\alpha$ -SNAP) in crayfish neurons. *A*: 150  $\mu$ g of detergent solubilized extracts from crayfish CNS and muscle and rat brain were separated by 10% SDS-PAGE and analyzed by Western blotting with a polyclonal anti- $\alpha$ -SNAP antibody. Immunodecorated proteins were detected with the appropriate secondary antibody conjugated to horseradish peroxidase and the enhanced chemiluminescence system. *B*: immunofluorescence staining of motor nerve terminals of the opener muscle was done with the same anti- $\alpha$ -SNAP antibody and a Texas-Red-conjugated secondary reagent. Both inhibitory and excitatory terminals show enhanced accumulation of  $\alpha$ -SNAP within the varicosities (arrows) in which pools of synaptic vesicles and synapses are located. Scale bar represents 25  $\mu\text{m}$ . *C*: visualization of the excitatory terminals loaded with a mixture of  $\alpha$ -SNAP and Texas Red dextran (70 kDa) after 30 min of pressure injection. Note only the excitatory terminals are loaded.

### Protein microinjection

Immediately before injection the proteins were mixed with a Texas Red dextran solution (70 kDa, Molecular Probes) to a final concentration of 0.51 mg/ml protein and 0.05% of Texas Red dextran. This solution then was loaded into the microelectrode by capillary action from the back of the electrode until the tip of the electrode was filled sufficiently so that the wire from the electrode holder touched the solution interface. The microelectrode then was placed into the excitatory axon of the opener muscle close to the axon bifurcation. Within 30 min of the start of pressure injections, the 70-kDa Texas Red dextran had entered nerve terminals and loaded the varicosities (Fig. 1C). Because the molecular weights of  $\alpha$ -SNAP and  $\alpha$ -SNAP(L294A) mutant are 35 kDa, it would be expected that they would have also diffused into the varicosities during this time. The membrane potential of the axon was in the range of  $-60$  to  $-70$  mV with this type of solution loaded into the electrode. To inject the protein, pressure was applied with a PicoSpritzer II (General Value, Fairfield, NJ) within a pressure range of 10–60 psi. The pressure was varied depending on how well the axon filled. Because the excitatory motor axon is stimulated selectively in the meropodite, only it will produce action potentials; therefore it is possible to confirm penetration of the excitatory axon by the microelectrode.

### Evoked postsynaptic potential measurements

Intracellular muscle recordings were made with a 3 M KCl-containing microelectrode placed in a centrally located fiber in the opener muscle (Fig. 2, A and B). The responses were amplified with a  $1 \times$  LU head stage and an Axoclamp 2A amplifier (Axon Instruments, Foster City, CA). Axons were stimulated by a train of 10 pulses given at the indicated frequencies. The stimulation frequency was kept constant for each preparation. The range in frequencies used varied from 40 to 60 Hz with a train interval of 10 s. The frequency chosen was determined at the time of the experiment to ensure an excitatory postsynaptic potential (EPSP) response by the fourth pulse of the train. Because the stimulus train is phase locked, one readily can measure each of the 10 peak amplitudes of the EPSPs and the sweep number in which they occurred. The sweep number, the mean value of the baseline, and the maximum of EPSP amplitudes were all recorded. All events were measured and calibrated with the MacLab Scope software 3.5.4 version (ADInstruments, Mountain View, CA). Stimulation was obtained using a Grass S-88 stimulator and a stimulation isolation unit (Grass Instruments, Warwick RI) with leads to a standard suction electrode (Cooper et al. 1995b).

To quantitatively compare the changes caused by the injected agents in the various preparations, the measurements were normalized to a percent change. The percent change from baseline was calculated using the difference among the average of the first 100 EPSP events during the baseline recording before injection and the average of the 100 EPSP events around the maximum response during the injection procedure and then dividing the result by the baseline value as shown in the following equation:  $[(\text{Baseline} - \text{maximum response})/\text{Baseline}] \times 100\% = \% \text{ Change}$ . The means of the calculated percent changes from baseline among preparations in which the carrier buffer only was injected into the axon, the  $\alpha$ -SNAP and the  $\alpha$ -SNAP(L294A) mutant were graphed for comparative purposes (Fig. 2C).

The 10th EPSP peaks of a train were used to calculate a facilitation index ( $Fe$ ) with respect to the earlier EPSP amplitudes (Crider and Cooper 1999). To calculate facilitation indices, the amplitude of the 10th EPSP was divided by one of the previous EPSP amplitudes and the result was subtracted from one. A facilitation index for each pulse in the train ( $X$ ) by the equation  $Fe_{(10/X)} = (10\text{th EPSP}/X\text{th EPSP}) - 1$ . The ratios were calculated for *events* 1–9 in each trial.

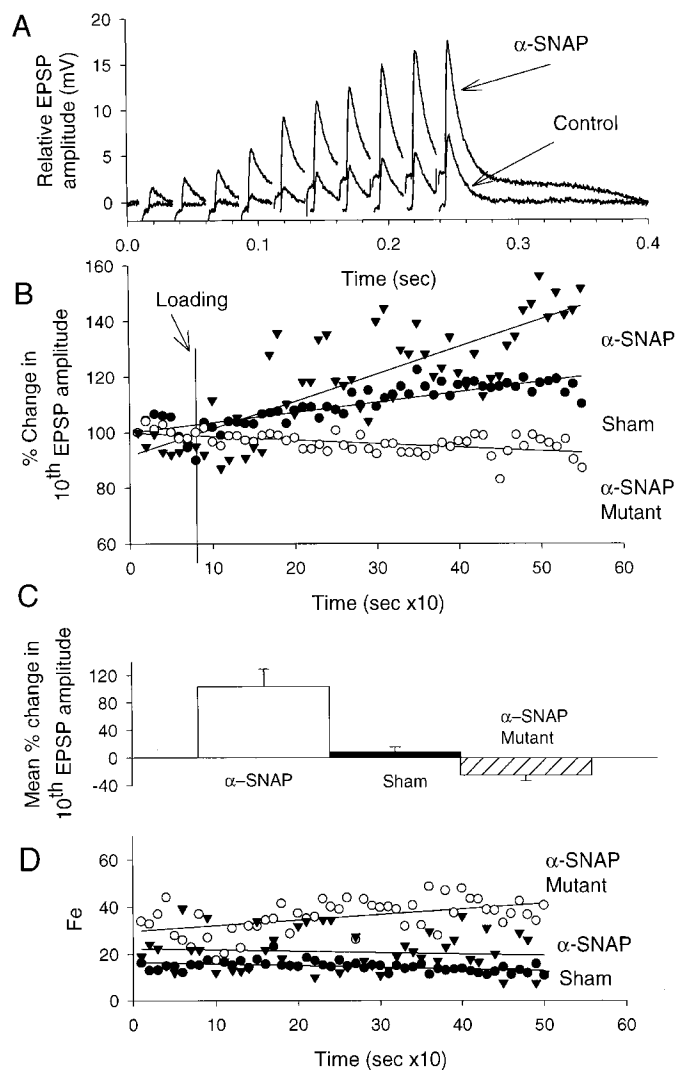


FIG. 2. Effect of  $\alpha$ -SNAP on evoked postsynaptic potentials (EPSPs). A: EPSPs from a train at 40-Hz stimulation for 250 ms before the start of injection (bottom) and after the terminals were well loaded with  $\alpha$ -SNAP (top). B: percent change in the 10th EPSP of a train was plotted vs. time of experiment for preparations loaded with  $\alpha$ -SNAP with Texas Red dextran, just Texas Red dextran with buffer (Sham), or the  $\alpha$ -SNAP(L294A) mutant with Texas Red dextran. To standardize the starting amplitude among the 3 preparations, the 10th EPSPs from the initial trains were set to 100%. Each point represents an average of 100 trains and interval among trains was 10 s. Vertical line (Loading) denotes the time at which the fluorescent dextran enter the nerve terminals. C: percent change in the mean ( $\pm$ SE) of the EPSP amplitudes before injection and at the peak of the response induced by each injection condition. An average of 100 10th EPSP amplitudes around the baseline and the maximum response values were used from each preparation. Percent change was calculated by the absolute value in the difference between the baseline and the maximum response, divided by the baseline and multiplied by 100%. D: to determine if the injection procedures had an influence on facilitation of transmitter release a facilitation index ( $Fe$ ) was calculated by the ratio of the amplitudes of 10th EPSP to the 1st EPSP, minus 1. When comparing  $Fe$  among all the preparations no significant increase was observed. Values shown are averages as mention for B.

### Excitatory postsynaptic current measurements

Focal macropatch recording was used to measure synaptic currents. The synaptic currents were obtained using the loose patch technique by lightly placing a 10- to 20- $\mu$ m diam, fire-polished, glass electrode directly over a single, spatially isolated varicosity along the vital dye-visualized nerve terminal. The macropatch electrode is specific

for current recordings within the region of the electrode lumen. The lumen of the patch electrode was filled with the same solution as the bathing medium, and the seal resistance was in the range of 100 kΩ to 1 MΩ. Because the seal can be lost easily if the muscle twitches under the electrode, stimulation was restricted to a range of 1–2.5 Hz. Evoked EPSCs (excitatory postsynaptic currents) and mEPSCs (miniature EPSCs) were recorded and analyzed to determine the mean quantal content ( $m$ ), the number of release sites ( $n$ ), and the average probability of release at a terminal ( $p$ ) (Cooper et al. 1995b, 1996b). In each synaptic current recording, a trigger artifact and a nerve spike can be visualized that indicates nerve stimulation. Mean quantal content can be determined by direct counts ( $m_{co}$ ): direct counts ( $m_{co}$ ) = [Σ (failures × 0), (single events × 1), (double events × 2) etc.]/total number of sweeps.

As shown in Fig. 3A, in some cases there were no evoked events that follow the nerve terminal spikes. This type of response is called a failure in evoked release, and is given the value of zero. If only one single event occurs after the spike, it is counted as a single-evoked event and is given the value of one (Fig. 3B). When double events occur, they are referred to as double-evoked events and are counted as two (Fig. 3C), etc.

The determination of quantal release over the time of the experiment is made possible by examining the area of the evoked current which is a measure of charge (Fig. 4). It should be noted that the time of peak evoked events varies due to latency jitter so the measurements of peak amplitude are not as reliable as the charge

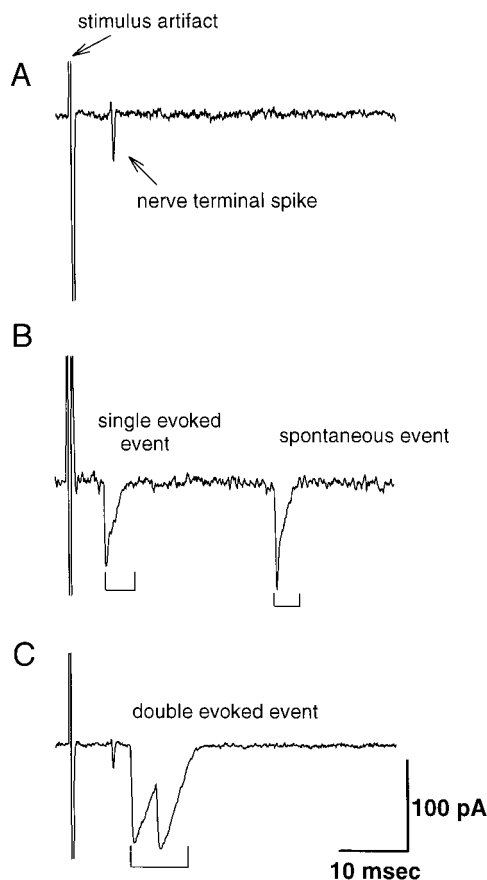


FIG. 3. Examples of synaptic quantal currents as measured with a focal macropatch electrode. A focal macropatch electrode was placed directly over individual varicosities and current traces were recorded after stimulation. Current traces are used to count the number of vesicles that are released per stimulus. In A, no release occurred and as a result this response is counted as a failure. In B, a single evoked event occurred with a spontaneous release shown later in the trace but with a very similar sized event. In C, a doublet of evoked events occurred that would be counted as 2 evoked events.

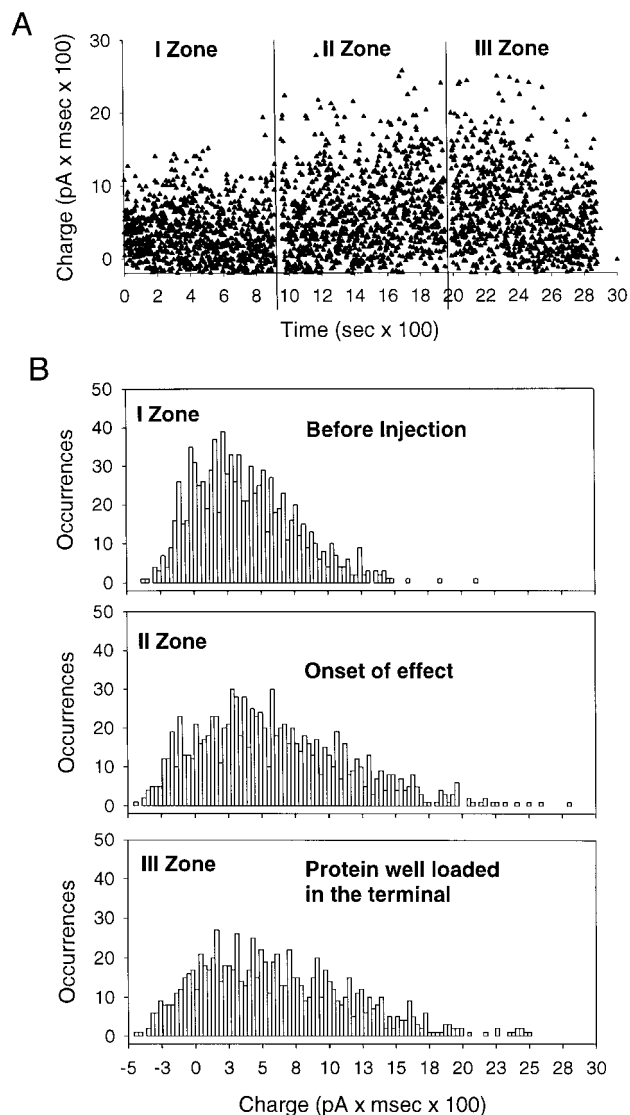


FIG. 4. Effect of α-SNAP on evoked release. Effect of microinjected α-SNAP is readily observed over time in a scatter graph of the synaptic charge as measured with a focal macropatch electrode (see Fig. 3). A: zone I, represents the baseline recording prior to injection. Zone II represent events that occurred as the dye starts to appear in the terminals, and zone III is when the dye becomes well loaded into the terminals. Shifts in the charge of the various evoked events were plotted as histograms of the 3 time zones in B.

measure when multiple events occur (Fig. 3C). The change in the charge measures before and after loading proteins in the nerve terminals and the histograms of the frequency in occurrence of charge of the evoked events were calculated. The data sets were tested for a best-fit approximation based on assumptions discussed in earlier reports (Cooper et al. 1995b; Wernig 1975). Binomial distributions are known to represent the quantal nature of release in crayfish neuromuscular junctions (Wojtowicz et al. 1991). To test for nonuniform binomial distributions, the procedures described earlier were used (Wojtowicz et al. 1991). The  $\chi^2$  statistic and a modified Akaike information criterion (AIC) were used to estimate the distribution that best fits the observed distribution of events. Because the injection of the protein produced gradual changes in all the quantal parameters, sample sets of data for every 400 events were used and were found to be sufficient to obtain statistically significant values for quantal predictions.

### Analysis of latency

Latency was measured as the time period between the starting point of the spike (extracellular recorded action potential) and starting point of evoked events (for the 1st and the 2nd events) (Fig. 6, A and B). A representative plot of the frequency of occurrence at various latencies is provided (Fig. 7A), and a normalized graph for the occurrence of events is shown for the two curves in Fig. 7B, as plotted in cumulative frequency for the latencies measured (i.e., Kolmogorov-Smirnov) (Zar 1999).

## RESULTS

### Presence of $\alpha$ -SNAP in crayfish neurons

Western blotting experiments confirmed the presence of  $\alpha$ -SNAP in crayfish neurons. Not surprisingly, the anti-bovine  $\alpha$ -SNAP antibody was able to cross-react with the crayfish SNAP. This is consistent with the high degree of sequence conservation between  $\alpha$ -SNAPs identified from a wide variety of species (e.g., *Drosophila* and bovine  $\alpha$ -SNAP are 61% identical) (Pallanck et al. 1995). The crayfish protein had a similar molecular weight to that of the rat protein (Fig. 1A), and comparable levels of protein were seen in rat brain and crayfish CNS. Immunofluorescence studies indicate that crayfish  $\alpha$ -SNAP is present in both excitatory and inhibitory motor neurons and appears concentrated in the nerve terminals. This is born out by the staining of the varicosities in Fig. 1B. Extensor muscles containing both phasic and tonic excitatory motor neurons also show neuronal staining with this antibody (data not shown). From these data, it appears that  $\alpha$ -SNAP is concentrated in the terminals of each of the two classes of motor neurons that innervate the crayfish muscle (Fig. 1C).

### Effects of $\alpha$ -SNAP on EPSP amplitudes

Measuring the change in EPSP amplitude readily can provide an indication of whether a microinjected protein alters NT release. To test the effect of  $\alpha$ -SNAP during injection, the axon was stimulated by a train of 10 pulses at 40 Hz with an interval of 10 s, and 10 EPSP responses were recorded by an intracellular electrode. As shown in Fig. 2A,  $\alpha$ -SNAP enhanced the amplitudes of the EPSPs. The superimposed graphs of evoked EPSPs for the control and  $\alpha$ -SNAP injected axons show that there is a consistent increase in the amplitudes. This enhancement of EPSP amplitude was most obvious at later stimulus events in the trains. For this reason, the 10th responses from each train were recorded versus time and plotted in Fig. 2B. (Although clearly not a linear function, a best-fit line was drawn through each data set to aid in comparisons.) Amplitude increases were seen only after the dye/ $\alpha$ -SNAP solution began to appear in the nerve terminal (denoted by the vertical line on Fig. 2B). The  $\alpha$ -SNAP(L294A) mutant had the opposite effect, causing a decrease in the EPSP amplitudes (Fig. 2B). This decrease initiated after the dye/protein entered the nerve terminals. The sham injections resulted in slight increase in the amplitudes of the EPSPs. This indicates that the injection process may have a positive effect on EPSP amplitude, suggesting that the effect of  $\alpha$ -SNAP may be slightly overestimated, whereas the inhibition by  $\alpha$ -SNAP(L294A) was slightly underestimated.

The changes in the EPSP amplitudes were normalized to a percent change, which was determined by the difference of the

average in the first 100 EPSPs events during the baseline and the average in the 100 EPSPs events around the maximum response (Fig. 2C). Although there was some variability in the percent change from preparation to preparation, it is clear that  $\alpha$ -SNAP causes an almost twofold increase in EPSP amplitude. The dominant negative mutant, however, was clearly inhibitory leading to a 20% decrease in the 10th EPSP peak amplitude. For the purpose of illustration, data obtained using the 10th EPSP are shown in Fig. 2C, yet in most preparations, the maximal effect of the injected proteins occurred between the 3rd and the 5th EPSP peaks of the stimulus train. When the 4th peaks were compared with sham injected, there was a two- to fourfold increase in EPSPs ( $n = 3$ ) when  $\alpha$ -SNAP was injected and a 45–80% decrease in EPSPs ( $n = 3$ ) when the mutant  $\alpha$ -SNAP was injected (data not shown). The fact that  $\alpha$ -SNAP has a positive effect on EPSP amplitude and the dominant negative  $\alpha$ -SNAP(L294A) mutant has an inhibitory effect suggests that the mammalian proteins are functional in the crayfish NMJ. This justifies the use of these proteins to study the role of  $\alpha$ -SNAP in NT release at these NMJs.

### $\alpha$ -SNAP does not affect facilitation of EPSPs

Facilitation, or the progressive increase of EPSP amplitude during the course of a train of stimuli, is thought to be indicative of a progressive increase in calcium concentration in the nerve terminal (Bain and Quastel 1992; Delaney et al. 1989). By measuring the effect of a microinjected protein on facilitation, one can assess the calcium requirement for that protein to act. The EPSP amplitudes for each event within a train were recorded during the entire injection period. A facilitation index for each pulse ( $X$ ) in the train was calculated by the equation  $Fe_{(10/X)} = (10\text{th EPSP}/X\text{th EPSP}) - 1$ . As an example of this type of analysis,  $Fe_{(10/1)}$  is plotted versus injection period time for the three different treatments (Fig. 2D). There was no change in  $Fe_{(10/X)}$  in any of the injection experiments when the numerous possible  $Fes$  were calculated. This indicates that EPSP amplitudes from the 1st event to the 10th event increased proportionally. These data demonstrate that neither  $\alpha$ -SNAP nor the mutant affect facilitation of NT release in the crayfish NMJ, suggesting that the role of  $\alpha$ -SNAP is not calcium dependent.

### $\alpha$ -SNAP effects on quantal release

$\alpha$ -SNAP increases the EPSP amplitudes of crayfish NMJ, consistent with its effect on squid axons described by DeBello et al. (1995). Taking advantage of the crayfish system, we turned to quantal analysis to determine the potential mechanisms by which  $\alpha$ -SNAP causes this increase. The crayfish NMJ is ideal for this type of analysis because its relatively low output allows single events to be monitored and statistical analysis to be applied. The number of evoked events and failures before (Zone I in Fig. 4) and during  $\alpha$ -SNAP injections (Zone II and III in Fig. 4) was counted directly, making sure to distinguish single events from multiple events (as delineated in Fig. 3). The evoked current over time (charge) was used to assess synaptic release and spontaneous events. The charge measure is a more appropriate measure than peak amplitudes because of the latency jitter in evoked release, and it allows the rates of release to

be determined. The evoked charge was enhanced as α-SNAP began to appear under the electrode (Fig. 4A, compare Zone I with II and III). Once the dye filled the nerve terminals, more evoked events were obtained and there was an increase in the charge of these events (Fig. 4A). The increase in evoked charge, after α-SNAP reached the terminals, is indicated by the rightward shift in the histogram distribution of the data set shown in Fig. 4B. Larger evoked charges and fewer failures were present after the protein was well loaded in the terminal (Fig. 4B, zone III).

α-SNAP affects not only the evoked charge but also the occurrences of evoked events and the number of failures. The numbers of failures decreased after the dye began to reach nerve terminals and were maintained at low levels throughout the injection period (Fig. 5A). The rate at which the failures occurred also decreased as the dye reached the terminals. The reduced failure rate stayed constant for the remainder of the experiment (Fig. 5B). This dampening of failure rate was common in the six preparations in which α-SNAP was injected.

Mean quantal content ( $m_{co}$ ) is the average number of evoked-release events per action potential. As shown in Table 1 for one experiment, α-SNAP injection leads to an increase in quantal content. This increase was seen in all six experiments, ranging from +7 to +124% relative to the uninjected control (Table 2). An increase in quantal content could be due to an increase in the number of release sites or to an increase in the number of release events per site. To distinguish between these

TABLE 1. Direct counts of quantal events and estimates of quantal parameters  $n$  and  $p$  in the presence of α-SNAP

Experiment	Events	Observed	Best Fit	$n$	$p$	Quantal Content ( $m$ )
Control						
0 s	0	334	341	1	0.15	0.185
	1	58	59			
	2	8	0			
400 s	0	363	365	1	0.09	0.098
	1	35	35			
	2	2	0			
800 s	0	339	340	1	0.15	0.155
	1	60	60			
	2	1	0			
1,200 s	0	335	335	2	0.08	0.165
	1	64	64			
	2	1	1			
1,600 s	0	334	334	2	0.08	0.173
	1	63	63			
	2	3	3			
α-SNAP						
2,000 s	0	334	334	2	0.09	0.170
	1	64	64			
	2	2	2			
2,400 s	0	328	327	2	0.095	0.205
	1	69	69			
	2	0	4			
	3	2	0			
2,800 s	0	325	330	1	0.17	0.200
	1	68	69			
	2	6	0			
	3	1	0			
3,200 s	0	295	295	2	0.15	0.315
	1	108	108			
	2	6	6			
	6	1	0			
3,600 s	0	321	321	2	0.10	0.213
	1	75	75			
	2	3	2			
	4	1	0			
4,000 s	0	340	341	1	0.15	0.150
	1	59	59			
	2	1	0			
4,400 s	0	355	278	2	0.16	0.128
	1	42	111			
	2	1	10			
	3	1	0			
	4	1	0			

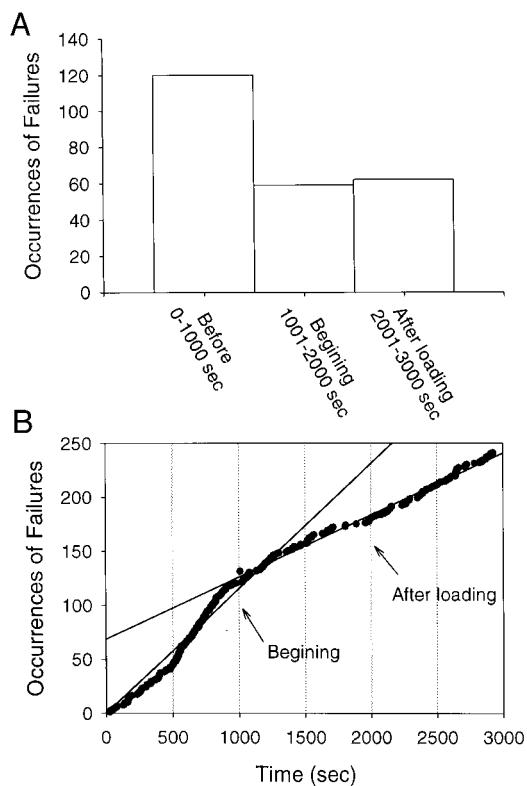


FIG. 5. Effect of α-SNAP on the number of failed evoked events. A: number of failed evoked events was totaled for 3 1,000-s periods: before injection (before), as dextran and α-SNAP entered the terminal (beginning), and once the terminal was loaded (after loading). B: rate at which the failures occurred during these periods was plotted as a linear function both before injection and after α-SNAP had reached the terminals.

The first column represents the recording conditions; the second column represents the number of discrete events (0, failures, 1, single events, 2, double events etc.) that occurred per sweep; and the third column represents the number of occurrences during the 400-s period. The quantal parameters ( $n$  and  $p$ ) are calculated from the best fit of the event distribution as determined by the MLE and bootstrapping procedures (See *Experimental procedures*). The  $p$  is the average probability value for the 400-s period data set. SNAP, soluble N-ethylmaleimide-sensitive factor attachment protein.

two possibilities, the total number of failures, single- and multiple-evoked events in 400 sweeps were combined, and the best fit of the data set distribution was calculated. From this analysis, the quantal parameters,  $n$  (number of release sites) and  $p$  (probability of release at a site), can be determined by the methods previously described (Cooper et al. 1995b). In Table 1, the  $p$  values represent an average value. Typically, injection of α-SNAP did not significantly change  $n$ , relative to sham injection, in any of the six preparations. However, α-SNAP injection consistently increased  $p$  ranging from +27 to +161%, relative to control (Table 2). These data indicate that

TABLE 2. Effect of  $\alpha$ -SNAP on the mean quantal content ( $m_{co}$ ) and  $p$  within a single varicosity

Preparation	$m_{co}$			$p$		
	Baseline	$\alpha$ -SNAP	% $\Delta$	Baseline	$\alpha$ -SNAP	% $\Delta$
1	0.145	0.325	+124	0.124	0.163	+32
2	0.221	0.315	+43	0.124	0.158	+27
3	0.155	0.315	+103	0.1096	0.147	+34
4	0.244	0.340	+39	0.102	0.266	+161
5	0.207	0.295	+43	0.103	NF*	—
6	0.233	0.250	+7	0.116	0.214	+85

The mean quantal content was determined by direct counts as indicated in Table 1. The values obtained for baseline is an average over the entire time before dye was observed in the terminals. The value listed for  $\alpha$ -SNAP is the maximum value within a group of 400 events as shown in Table 1. The percent change (% $\Delta$ ) was determined by taking the absolute difference among baseline and  $\alpha$ -SNAP maximum and dividing the result by the baseline value, followed by multiplication by 100. \*NF indicates that there was insufficient data to determine a satisfactory curve fit of the distribution.

$\alpha$ -SNAP increases the probability of release at a site but does not increase the number of release sites.

#### Effect of $\alpha$ -SNAP on latency

Latency is defined as the time required for an action potential to induce NT release. In molecular terms, it is the time required for a primed and docked SV to respond to the calcium influx and fuse with the active zone. Measuring from the starting point of the spike to the starting point of an evoked event in the EPSC records, it is possible to calculate the time needed for an evoked event to occur (Fig. 6). In the crayfish NMJ, the fastest events took  $\sim$ 1–2 ms. After injection of  $\alpha$ -SNAP the fastest events stayed the same but more of these

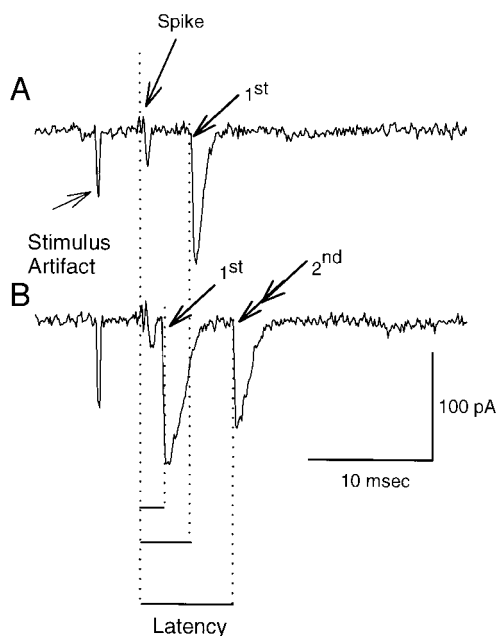


FIG. 6. Examples of synaptic latency measurements. Synaptic latency is measured as the time from when the action potential reaches the nerve terminal until the time the postsynaptic currents are measured. In practice, that is the time between the start of the poststimulus spike and the start of the response current. In A, the latency is longer for the 1st event than in B, but the 2nd evoked event in B has a longer latency than the 1st events for either trace.

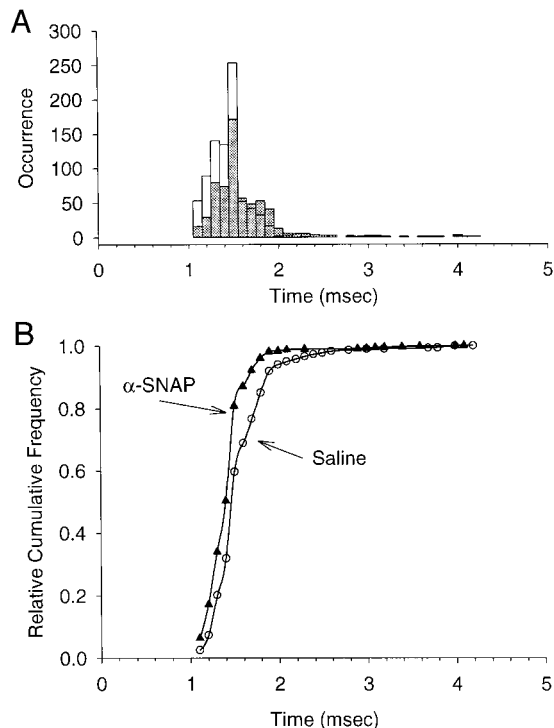


FIG. 7. Effect of  $\alpha$ -SNAP on latency. Occurrence of 1st evoked events with the indicated latencies is depicted in the histogram in A with  $\blacksquare$  representing the control and  $\square$  representing  $\alpha$ -SNAP-injected terminals. Because more events occur in the presence of  $\alpha$ -SNAP, the effects on the occurrence of various latencies were normalized and cumulative frequency plots was made. B: leftward shift in the curve representing  $\alpha$ -SNAP indicates that more vesicles are releasing at earlier times with the minimum time for release remaining the same. This leftward shift was observed in 6 of the 6 preparations analyzed.

fast events occurred. The superimposed histograms in Fig. 7A indicate that more events had shorter latencies after  $\alpha$ -SNAP was loaded into the terminals. Synaptic vesicular fusion rates became apparently faster because more vesicles were “releasable” in the presence of  $\alpha$ -SNAP, thus the larger amplitude bins in the histograms (Fig. 7A). Because there are more events occurring, it is hard to visualize if there is a leftward shift in the histogram or if the difference is just due to more events. Because of this ambiguity, the latency was normalized into cumulative frequency plots (Fig. 7B). From this analysis of the data, it becomes more obvious that there is a slight leftward shift (decrease in latency) as more events occur at an earlier time throughout the normalized distribution. Presumably the larger number of releases indicates that more quanta are releasable. However, shift in the histogram would simply indicate that slower releases are sped up. These “slowly released” quanta are releasable, but they might be released more rapidly in the presence of  $\alpha$ -SNAP. This trend was seen in six different preparations injected with  $\alpha$ -SNAP.

#### DISCUSSION

In summary, the results presented here suggest that the role of  $\alpha$ -SNAP in the synapse is to increase the pool of “readily releasable” synaptic vesicles. This is supported by several observations. Initially, microinjection of  $\alpha$ -SNAP caused an increase in synaptic output (Fig. 2) and NT release could be inhibited by the dominant negative  $\alpha$ -SNAP(L294A) mutant.

Neither protein had an effect on facilitation (Fig. 2D), indicating that  $\alpha$ -SNAP did not alter calcium buffering or loading within the terminal, and thus calcium channels were unaffected by the protein injections. Quantal analysis of the effects of microinjected  $\alpha$ -SNAP showed that it caused a decrease in the failure rate of NT release (Figs. 4 and 5) and led to a slight decrease in release latency (Fig. 7).  $\alpha$ -SNAP did not accelerate the minimal process required for SV fusion but increased the availability of vesicle for release at the maximum rates (Fig. 7B). These findings suggest that  $\alpha$ -SNAP causes an increase in the fusion competence of SVs without significantly effecting NT release kinetics. This is supported further by statistical analysis of the quantal data (Tables 1 and 2). From this analysis, it is clear that  $\alpha$ -SNAP serves to increase the probability ( $P$ ) that a stimulus will result in a release event but it does not significantly increase the number of sites ( $n$ ) at which release can occur. Mechanistically, these data support the model in which SNAPs (and perhaps by extension NSF) are involved in increasing the pool of fusion competent SVs but are not involved in the actual membrane fusion events. Because transmitter release was inhibited by the dominant negative  $\alpha$ -SNAP(L294A) mutant, it appears that the mutant competed for interaction of the native  $\alpha$ -SNAP, which is likely present in much lower amounts than the injected mutant  $\alpha$ -SNAP. The effects were gradual and increased with injection time, suggesting a selective interaction and not a massive nondirected protein interaction on ionic channels or on other aspects of the release machinery.

The low output tonic motor nerve terminals of the crayfish makes it an effective preparation to address questions related to the kinetics and mechanics of synaptic transmission because latency measurements and quantal analysis can be performed readily. This type of analysis, available with the crayfish NMJ, is not feasible in higher output synapses such as the squid giant synapse and the *Drosophila* NMJ or among vertebrate neurons in culture. The low output of tonic motor nerve terminals is partly due to the synaptic ultrastructure because these synapses may contain one or a few active zones where evoked release can occur. This architecture results in a relatively simple synaptic structure to investigate alterations in the number of vesicles docked around an active zone by electron microscopy studies. Likewise physiological measures of small changes in synaptic efficacy can be quantified to assess manipulations of the release machinery.

We addressed potential mechanisms in  $\alpha$ -SNAP function by examining the quantal parameters and by determining if the timing of evoked events is altered. This tonic low-output motor nerve terminal is ideal for this study because it normally shows latency jitter as indicated by the range of times between depolarization and vesicle release. By measuring the latencies of the first evoked events before and during  $\alpha$ -SNAP injections, one can determine if the mechanics of vesicle docking/priming are altered. Because the number of events also increases along with more events occurring with a shorter latency, histograms of the occurrence of events at various times (Fig. 7A) is not of particular use. The relative cumulative graphs of latency are more beneficial for determining shifts in the latency but the shifts only can be observed within data sets because the cumulative graphs are first-rank summed to measure relative differences (Fig. 7B). Groups of 400 evoked trials were compared before and during injections of  $\alpha$ -SNAP. After the ter-

minals began to be loaded with  $\alpha$ -SNAP, no further shifts were detected among the groups of data sets. The shifting of the vesicle pool to minimum release times reveals that an increase in  $\alpha$ -SNAP at the terminal promotes the fusion competence of vesicles but does not effect the time required for the  $\text{Ca}^{2+}$ -influx-induced membrane fusion process, which is consistent with earlier work in neurons (DeBello et al. 1995) and endocrine cells (Kibble et al. 1996; Martin et al. 1995). Only ultrastructural analysis after rapid fixation and subsequent serial sectioning of the synapses would allow one to prove such a postulation anatomically. The physiological data suggest that  $\alpha$ -SNAP is working to enhance vesicle docking/priming. With the methods used in this study, we are not able to assess whether  $\alpha$ -SNAP also plays a role in vesicle recycling as might be inferred from the demonstration of a role for NSF in this process (Littleton et al. 1998).

Several aspects can contribute to the diversity of NT release by nerve terminals. Ultrastructural analysis of nerve terminals suggest that there is great deal of heterogeneity in the number of vesicles that can encircle the active zones of the synapses (Govind et al. 1994). This suggests that various number of vesicles could be primed for release in each active zone; however, the conformational constraints of the active zone suggest that there may be a limit to the total number of primed/docked vesicles possible. Also, depending on the synaptic complexity (Cooper et al. 1996b,c; King et al. 1996; Msghina et al. 1998), multiple active zones may be present on a single synapse, thus providing a structural basis for synaptic differentiation to effect synaptic efficacy. These structural arrangements of active zones could allow for a fine-tuning of neurotransmission by specific neurons. Additionally, cytoplasmic proteins such as  $\alpha$ -SNAP could provide a mechanism for fine-tuning synaptic efficacy at the established active zones. This could be accomplished by regulating the level of expression or of axonal transport of these proteins. Because microinjected  $\alpha$ -SNAP does increase NT release in both squid axons (DeBello et al. 1995) and in crayfish NMJs, it seems simple up- or downregulation of SNAP levels at the synapse could be used to modulate NT release. Alternatively, there are other plausible mechanisms that could facilitate vesicle docking/priming to control the efficacy of NT release. The effect of stimulation on protein phosphorylation events is a viable mechanism because it is well known that the entry of calcium can lead to the activation of various protein kinases such as protein kinase C and calmodulin kinase II (Makhinson et al. 1999; Valtorta et al. 1996). For example, phosphorylation of synapsins by the calcium-activated kinases has been shown to increase the pool of free SVs by facilitating their release from the presynaptic cytoskeleton (Benfenati et al. 1992). Several other studies have shown the elements of the synaptic secretory machinery can be phosphorylated in vitro [e.g., Munc18/nSec1 (Fujita et al. 1996; Shuang et al. 1998), SNAP-25 (Risinger and Bennett 1999; Shimazaki et al. 1996), synaptophysin (Barnekow et al. 1990; Rubenstein et al. 1993), and synaptotagmin (Bennett et al. 1993; Davletov et al. 1993; Popoli 1993)] and that phosphorylation affects their interactions with other secretory machinery components. Although all of these are possible mechanisms to control synaptic efficiency, detailed experiments are needed to address their relative importance in causing enhanced synaptic release during short- and long-term synaptic facilitation (Delaney et al. 1991; Dixon and Atwood 1989a,b;

Dudel et al. 1983; Parnas et al. 1982; Zucker and Fogelson 1986) and among terminals that show differences in synaptic efficacy (Atwood and Cooper 1995, 1996a,b; Atwood and Wojtowicz 1986; Atwood et al. 1994; Bradacs et al. 1997; Cooper et al. 1998; King et al. 1996; LaFramboise et al. 1999).

The stochastically derived quantal parameters  $n$  and  $p$ , are to help one determine possible mechanisms but because the calculated  $n$  is difficult to directly correlate to a structural identity, it remains open for debate if much weight can be placed on such indices for a structural meaning. Latency, facilitation measures, and direct quantal counts for the calculation of  $m$  are not as subjective indices as  $n$  and  $p$ , and thus are emphasized in this report. It is beyond the scope of this report to dwell on the finer points of quantal analysis but to highlight a few points may clarify the reason of not placing to much emphasis on  $n$  and  $p$  for mechanistic interpretations here or in future descriptions. The synaptic structure of the crayfish neuromuscular junction is one in which multiple vesicles can dock around an dense body (i.e., an active zone); in addition, a synapse can have multiple active zones with varied spacing between them (Cooper et al. 1995a, 1996c). So the problem with a structural interpretation of  $n$  is that  $n$  maybe inferred to be the various numbers of docking sites around a single active zone or each active zone itself. In vertebrate synaptology,  $n$  is interpreted to represent an entire bouton or varicosity that contains multiple synapses with each synapse containing multiple active zones (Korn et al. 1981). At least with the simplest of the crustacean synapses and the structural reconstructions of recorded varicosities (Atwood and Cooper 1996a,b; Atwood et al. 1994; Cooper et al. 1995a, 1996c), an anatomic meaning for  $n$  may be forthcoming when better stochastic analysis can be performed when synaptic efficacy is altered experimentally. For now, if one allows  $n$  to represent a single active zone, injection of  $\alpha$ -SNAP would likely enhance the number of docked vesicles within each single active zone, thus increasing the probability that each would release a single quantum. But if the same active zones are being used, then only  $p$  will increase and  $n$  would remain constant. If additional active zones were recruited at the same stimulation frequency used for the analysis, then  $n$  would increase. In that case, however, it is likely that  $p$ , which represents the average probability of release, would decrease. Because the  $p$  values reported are average  $p$ 's, when  $n$  increases  $p$  may decrease, unless of course  $p$  increases to such an extent that it is still larger after the division of  $n$ . The fact that we measured an increase in  $p$  with the stimulation paradigm used suggests the same active zones were used with an enhanced probability of release. These active zones are likely the ones in close concert with neighboring active zones on a single synapse (see Cooper et al. 1996c for the computational interpretations). One would predict that  $n$  would increase with an increase in the presence of  $\alpha$ -SNAP, and this likely may be seen when quantal assessment can be performed with accuracy at higher stimulation frequencies, but at present we do not feel that the analysis can accurately be performed when  $n$  is  $>3$  (personal conversation with Dr. Bruce Smith developer of the quantal analysis software used, Dalhousie University, Canada), and therefore we did not assess substantially higher

stimulation frequencies while increasing the amount of  $\alpha$ -SNAP within the terminals.

What is clearly demonstrated in this paper is that  $\alpha$ -SNAP does increase synaptic output by increasing the probability that a stimulus will result in NT release. On cellular terms, this suggests that  $\alpha$ -SNAP increases the ready release pool of fusion competent SVs. On a molecular basis, we must assume that  $\alpha$ -SNAP is effecting NT release by acting on the SNARE proteins present in the active zone and SVs, though that was not specifically addressed here. This would imply that  $\alpha$ -SNAP functions not in the fusion event but before calcium influxes to induce an activated conformation in the SNARE proteins so that they are primed to participate in membrane fusion.

Funding for this research was provided by the University of Kentucky Research and Graduate Studies Office (R. L. Cooper), National Science Foundation Grant IBN-9808631 (R. L. Cooper) and NSF-ILI-DUE 9850907 (R. L. Cooper) as well as an undergraduate training fellowship from Howard Hughes Medical Institute (R. C. Southard), and National Heart Lung, and Blood Institute Grant HL-56652 (S. W. Whiteheart).

Address for reprint requests: R. L. Cooper, T. H. Morgan School of Biological Sciences, 101 Morgan Bldg., University of Kentucky, Lexington, KY 40506-0225.

Received 3 June 1999; accepted in final form 2 September 1999.

#### REFERENCES

- ATWOOD, H. L. AND COOPER, R. L. Functional and structural parallels in crustacean and *Drosophila* neuromuscular systems. *Am. Zool.* 35: 556–565, 1995.
- ATWOOD, H. L. AND COOPER, R. L. Assessing ultrastructure of crustacean and insect neuromuscular junctions. *J. Neurosci. Methods.* 69: 51–58, 1996a.
- ATWOOD, H. L. AND COOPER, R. L. Synaptic diversity and differentiation: Crustacean neuromuscular junctions. *Invertebr. Neurosci.* 1: 291–307, 1996b.
- ATWOOD, H. L., COOPER, R. L., AND WOJTIOWICZ, J. M. Non-uniformity and plasticity of quantal release at crustacean motor nerve terminals. In: *Advances in Second Messenger and Phosphoprotein Research. Molecular and Cellular Mechanisms of Neurotransmitter Release*, edited by L. Stjärne, P. Greengard, S. E. Grillner, T.G.M. Hökfelt, and D. R. Ottoson. New York: Raven Press: 1994, 363–382.
- ATWOOD, H. L. AND WOJTIOWICZ, J. M. Short-term plasticity and physiological differentiation of crustacean motor synapses. *Int. Rev. Neurobiol.* 28: 275–362, 1986.
- BAIN, A. I. AND QUASTEL, D. M. Multiplicative and additive  $\text{Ca}^{2+}$ -dependent components of facilitation at mouse endplates. *J. Physiol. (Lond.)* 455: 383–405, 1992.
- BAJALIEH, S. M. AND SCHELLER, R. H. The biochemistry of neurotransmitter secretion. *J. Biol. Chem.* 270: 1971–1974, 1995.
- BANERJEE, A., BARRY, V. A., DASGUPTA, B. R., AND MARTIN, T.F.J. N-Ethylmaleimide-sensitive factor acts at a prefusion ATP-dependent step in  $\text{Ca}^{2+}$ -activated exocytosis. *J. Biol. Chem.* 271: 20223–20226, 1996.
- BARNARD, R. J., MORGAN, A., AND BURGOYNE, R. D. Stimulation of NSF ATPase activity by alpha-SNAP is required for SNARE complex disassembly and exocytosis. *J. Cell Biol.* 139: 875–883, 1997.
- BARNEKOW, A., JAHN, R., AND SCHARTL, M. Synaptophysin: a substrate for the protein tyrosine kinase pp60c-src in intact synaptic vesicles. *Oncogene* 5: 1019–1024, 1990.
- BENFENATI, F., VALTORTA, F., CHEREGATTI, E., AND GREENGARD, P. Interaction of free and synaptic vesicle-bound synapsin I with F-actin. *Neuron* 8: 377–386, 1992.
- BENNETT, M. K., MILLER, K. G., AND SCHELLER, R. H. Casein kinase II phosphorylates the synaptic vesicle protein p65. *J. Neurosci.* 13: 1701–1707, 1993.
- BRADACS, H., COOPER, R. L., MSGHINA, M., AND ATWOOD, H. L. Differential physiology and morphology of phasic and tonic motor axons in a crayfish limb extensor muscle. *J. Exp. Biol.* 200: 677–691, 1997.
- CLARY, D. O., GRIFF, I. C., AND ROTHMAN, J. E. SNAPS, a family of NSF attachment proteins involved in intracellular membrane fusion in animals and yeast. *Cell* 61: 709–721, 1990.

- COOPER, R. L. Development of sensory processes during limb regeneration in adult crayfish. *J. Exp. Biol.* 201: 1745–1752, 1998.
- COOPER, R. L., HAMPSON, D., AND ATWOOD, H. L. Synaptotagmin-like expression in the motor nerve terminals of crayfish. *Brain Res.* 703: 214–216, 1996a.
- COOPER, R. L., HARRINGTON, C. C., MARIN, L., AND ATWOOD, H. L. Quantal release at visualized terminals of a crayfish motor axon: intraterminal and regional differences. *J. Comp. Neurol.* 375: 583–600, 1996b.
- COOPER, R. L., MARIN, L., AND ATWOOD, H. L. Synaptic differentiation of a single motor neuron: conjoint definition of transmitter release, presynaptic calcium signals, and ultrastructure. *J. Neurosci.* 15: 4209–4222, 1995a.
- COOPER, R. L. AND RUFFNER, M. E. Depression of synaptic efficacy at intermolt in crayfish neuromuscular junctions by 20-hydroxyecdysone, a molting hormone. *J. Neurophysiol.* 79: 1931–1941, 1998.
- COOPER, R. L., STEWART, B. A., WOJTCWICZ, J. M., WANG, S., AND ATWOOD, H. L. Quantal measurement and analysis methods compared for crayfish and *Drosophila* neuromuscular junctions, and rat hippocampus. *J. Neurosci. Methods* 61: 67–78, 1995b.
- COOPER, R. L., WARREN, W. M., AND ASHBY, H. E. Activity of phasic motor neurons partially transforms the neuronal and muscle phenotype to a tonic-like state. *Muscle Nerve* 21: 921–931, 1998.
- COOPER, R. L., WINSLOW, J. L., GOVIND, C. K., AND ATWOOD, H. L. Synaptic structural complexity as a factor enhancing probability of calcium-mediated transmitter release. *J. Neurophysiol.* 75: 2451–2466, 1996c.
- CRIDER, M. E. AND COOPER, R. L. Importance of stimulation paradigm in determining facilitation and effects of neuromodulation. *Brain Res.* 842: 324–331, 1999.
- DAVLETOV, B., SONTAG, J. M., HATA, Y., PETRENKO, A. G., FYKSE, E. M., JAHN, R., AND SUDHOF, T. C. Phosphorylation of synaptotagmin I by casein kinase II. *J. Biol. Chem.* 268: 6816–6822, 1993.
- DEBELLO, W. M., O'CONNOR, V., DRESBACH, T., WHITEHEART, S. W., WANG, S. S., SCHWEIZER, F. E., BETZ, H., ROTHMAN, J. E., AND AUGUSTINE, G. J. SNAP-mediated protein-protein interactions essential for neurotransmitter release. *Nature* 373: 626–630, 1995.
- DELANEY, K., TANK, D. W., AND ZUCKER, R. S. Presynaptic calcium and serotonin-mediated enhancement of transmitter release at crayfish neuromuscular junction. *J. Neurosci.* 11: 2631–2643, 1991.
- DELANEY, K. R., ZUCKER, R. S., AND TANK, D. W. Calcium in motor nerve terminals associated with posttetanic potentiation. *J. Neurosci.* 9: 3558–3567, 1989.
- DIXON, D. AND ATWOOD, H. L. Adenylyl cyclase system is essential for long-term facilitation at the crayfish neuromuscular junction. *J. Neurosci.* 9: 4246–4252, 1989a.
- DIXON, D. AND ATWOOD, H. L. Conjoint action of phosphoinositol and adenylyl cyclase systems in serotonin-induced facilitation at the crayfish neuromuscular junction. *J. Neurophysiol.* 62: 1251–1259, 1989b.
- DUDEL, J. AND KUFFLER, S. W. The quantal nature of transmission and spontaneous miniature potentials at the crayfish neuromuscular junction. *J. Physiol. (Lond.)* 155: 514–529, 1961.
- DUDEL, J., PARNAS, I., AND PARNAS, H. Neurotransmitter release and its facilitation in crayfish muscle. VI. Release determined by both, intracellular calcium concentration and depolarization of the nerve terminal. *Pflügers Arch.* 399: 1–10, 1983.
- FUJITA, Y., SASAKI, T., FUKUI, K., KOTANI, H., KIMURA, T., HATA, Y., SUDHOF, T. C., SCHELLER, R. H., AND TAKAI, Y. Phosphorylation of Munc-18/n-Sec1/rbSec1 by protein kinase C: its implication in regulating the interaction of Munc-18/n-Sec1/rbSec1 with syntaxin. *J. Biol. Chem.* 271: 7265–7268, 1996.
- GOVIND, C. K., PEARCE, J., WOJTCWICZ, J. M., AND ATWOOD, H. L. “Strong” and “weak” synaptic differentiation in the crayfish opener muscle: structural correlates. *Synapse* 16: 45–58, 1994.
- HAAS, A. AND WICKNER, W. Homotypic vacuole fusion requires Sec17p (yeast  $\alpha$ -SNAP) and Sec18p (yeast NSF). *EMBO J.* 15: 3296–3305, 1996.
- HAY, J. C. AND MARTIN, T. F. Resolution of regulated secretion into sequential MgATP-dependent and calcium-dependent stages mediated by distinct cytosolic proteins. *J. Cell. Biol.* 119: 139–151, 1992.
- HE, P., WHITEHEART, S. W., PORTER, J. D., AND COOPER, R. L. Immunohistochemistry identification and assessment of the physiological role of synaptic vesicle docking related proteins,  $\alpha$ -SNAP and  $\gamma$ -SNAP at the crayfish NMJ. *Soc. Neurosci. Abstr.* 2: 148.9, 1997.
- HUNT, J. M., BOMMERT, K., CHARLTON, M. P., KISTNER, A., HABERMANN, E., AUGUSTINE, G. J., AND BETZ, H. A post-docking role for synaptobrevin in synaptic vesicle fusion. *Neuron* 12: 1269–1279, 1994.
- KAWASAKI, F., MATTIUIZ, A. M., AND ORDWAY, R. W. Synaptic physiology and ultrastructure in comatose mutants define an in vivo role for NSF in neurotransmitter release. *J. Neurosci.* 18: 10241–10249, 1998.
- KIBBLE, A. V., BARNARD, R. J., AND BURGOYNE, R. D. Patch-clamp capacitance analysis of the effects of  $\alpha$ -SNAP on exocytosis in adrenal chromaffin cells. *J. Cell Sci.* 109: 2417–2422, 1996.
- KING, M. J., ATWOOD, H. L., AND GOVIND, C. K. Structural features of crayfish phasic and tonic neuromuscular terminals. *J. Comp. Neurol.* 372: 618–626, 1996.
- KORN, H., TRILLER, A., MALLET, A., AND FABER, D. S. Fluctuating responses at central synapse:  $n$  of binomial fits predicts number of stained presynaptic boutons. *Science* 213: 898–901, 1981.
- LAFRAMBOISE, W., GRIFFIS, B., BONNER, P., WARREN, W., SCALISE, D., GUTHRIE, R. D., AND COOPER, R. L. Muscle type-specific myosin isoforms in crustacean muscle. *J. Exp. Zool.* 286: 36–48, 1999.
- LITTLETON, J. T., CHAPMAN, E. R., KREBER, R., GARMENT, M. B., CARLSON, S. D., AND GANETZKY, B. Temperature-sensitive paralytic mutations demonstrate that synaptic exocytosis requires SNARE complex assembly and disassembly. *Neuron* 21: 401–413, 1998.
- MAKHINSON, M., CHOTINER, J. K., WALTSON, J. B., AND O'DELL, T. J. Adenylyl cyclase activation modulate activity-dependent changes in synaptic strength and  $\text{Ca}^{2+}$ /calmodulin-dependent kinase II autophosphorylation. *J. Neurosci.* 19: 2500–2510, 1999.
- MARTIN, T.F.J. Stages of regulated exocytosis. *Trends Cell Biol.* 7: 271–276, 1997.
- MARTIN, T. F., HAY, J. C., BANERJEE, A., BARRY, V. A., ANN, K., YOM, H. C., PORTER, B. W., AND KOWALCHYK, J. A. Late ATP-dependent and  $\text{Ca}^{2+}$ -activated steps of dense core granule exocytosis. *Cold Spring Harbor Symp. Quant. Biol.* 60: 197–204, 1995.
- MAYER, A. AND WICKNER, W. Docking of yeast vacuoles is catalyzed by the Ras-like GTPase Ypt7p after symmetric priming by Sec18p (NSF). *J. Cell. Biol.* 136: 307–317, 1997.
- MAYER, A., WICKNER, W., AND HAAS, A. Sec18p (NSF)-driven release of Sec17p ( $\alpha$ -SNAP) can precede docking and fusion of yeast vacuoles. *Cell* 85: 83–94, 1996.
- MSGHINA, M., GOVIND, C. K., AND ATWOOD, H. L. Synaptic structure and transmitter release in crustacean phasic and tonic motor neurons. *J. Neurosci.* 18: 1374–1382, 1998.
- NAGIEC, E. E., BERNSTEIN, A., AND WHITEHEART, S. W. Each domain of the N-ethylmaleimide-sensitive fusion protein contributes to its transport activity. *J. Biol. Chem.* 270: 29182–29188, 1995.
- PALLANCK, L., ORDWAY, R. W., RAMASWAMI, M., CHI, W. Y., KRISHNAN, K. S., AND GANETZKY, B. Distinct roles for N-ethylmaleimide-sensitive fusion protein (NSF) suggested by the identification of a second *Drosophila* NSF homologue. *J. Biol. Chem.* 270: 18742–18744, 1995.
- PARNAS, H., DUDEL, J., AND PARNAS, I. Neurotransmitter release and its facilitation in crayfish. I. Saturation kinetics of release, and if entry and removal of calcium. *Pflügers Arch.* 393: 1–14, 1982.
- POIRIER, M. A., XIAO, W., MACOSKO, J. C., CHAN, C., SHIN, Y. K., AND BENNETT, M. K. The synaptic SNARE complex is a parallel four-stranded helical bundle. *Nat. Struct. Biol.* 5: 765–769, 1998.
- POPOLI, M. Synaptotagmin is endogenously phosphorylated by  $\text{Ca}^{2+}$ /calmodulin protein kinase II in synaptic vesicles. *FEBS Lett.* 317: 85–88, 1993.
- RISINGER, C. AND BENNETT, M. K. Differential phosphorylation of syntaxin and synaptosome-associated protein of 25 kDa (SNAP-25) isoforms. *J. Neurochem.* 72: 614–624, 1999.
- ROTHMAN, J. E. Mechanisms of intracellular protein transport. *Nature* 372: 55–63, 1994.
- RUBENSTEIN, J. L., GREENGARD, P., AND CZERNIK, A. J. Calcium-dependent serine phosphorylation of synaptophysin. *Synapse* 13: 161–172, 1993.
- SCHWEIZER, F. E., DRESBACH, T., DEBELLO, W. M., O'CONNOR, V., AUGUSTINE, G. J., AND BETZ, H. Regulation of neurotransmitter release kinetics by NSF. *Science* 279: 1203–1206, 1998.
- SHIMAZAKI, Y., NISHIKI, T., OMORI, A., SEKIGUCHI, M., KAMATA, Y., KOZAKI, S., AND TAKAHASHI, M. Phosphorylation of 25-kDa synaptosome-associated protein. Possible involvement in protein kinase C-mediated regulation of neurotransmitter release. *J. Biol. Chem.* 271: 14548–14553, 1996.
- SHUANG, R., ZHANG, L., FLETCHER, A., GROBLEWSKI, G. E., PEVSNER, J., AND STUENKEL, E. L. Regulation of Munc-18/syntaxin 1A interaction by cyclin-dependent kinase 5 in nerve endings. *J. Biol. Chem.* 273: 4957–4966, 1998.
- SIDDIQI, O. AND BENZER, S. Neurophysiological defects in temperature-sensitive paralytic mutants of *Drosophila melanogaster*. *Proc. Natl. Acad. Sci. USA* 73: 3253–3257, 1976.

- SOUTHARD, R. C., WINSLOW, J. L., HE, P., CHEN, D., WHITEHEART, S. W., AND COOPER, R. L. Influence of neuromodulators and vesicle docking related proteins on the kinetics of vesicular release. *Soc. Neurosci. Abstr.* 24: 327.10, 1998.
- SUDHOF, T. C. The synaptic vesicle cycle: a cascade of protein-protein interactions. *Nature* 375: 645–653, 1995.
- SUTTON, R. B., FASSHAUER, D., JAHN, R., AND BRUNGER, A. Crystal structure of a SNARE complex involved in synaptic exocytosis at 2.4 Å resolution. *Nature* 395: 347–353, 1998.
- TOLAR, L. A. AND PALLANCK, L. NSF function in neurotransmitter release involves rearrangement of the SNARE complex downstream of synaptic vesicle docking. *J. Neurosci.* 18: 10250–10256, 1998.
- VALTORTA, E., BENFENATI, F., AND BASUDEV, H. Role of protein kinases in nerve terminal maturation and function. *Biochem. Soc. Trans.* 24: 645–653, 1996.
- WEBER, T., ZEMELMAN, B. V., MCNEW, J. A., WESTERMANN, B., GMACHL, M., PARLATI, F., SOLLNER, T. H., AND ROTHMAN, J. E. SNAREpins: minimal machinery for membrane fusion. *Cell* 92: 759–772, 1998.
- WEIDMAN, P. J., MELANCON, P., BLOCK, M. R., AND ROTHMAN, J. E. Binding of an N-ethylmaleimide-sensitive fusion protein to Golgi membranes requires both a soluble protein(s) and an integral membrane receptor. *J. Cell. Biol.* 108: 1589–1596, 1989.
- WERNIG, A. Estimates of statistical release parameters from crayfish and frog neuromuscular junctions. *J. Physiol. (Lond.)* 244: 207–221, 1975.
- WHITEHEART, S. W., BRUNNER, M., WILSON, D. W., WIEDMANN, M., AND ROTHMAN, J. E. Soluble N-ethylmaleimide-sensitive fusion attachment proteins (SNAPs) bind to a multi-SNAP receptor complex in Golgi membranes. *J. Biol. Chem.* 267: 12239–12243, 1992.
- WHITEHEART, S. W., GRIFF, I. C., BRUNNER, M., CLARY, D. O., MAYER, T., BUHROW, S. A., AND ROTHMAN, J. E. SNAP family of NSF attachment proteins includes a brain-specific isoform. *Nature* 362: 353–355, 1993.
- WOJOWICZ, J. M., SMITH, B. R., AND ATWOOD, H. L. Activity-dependent recruitment of silent synapses. *Ann. NY Acad. Sci.* 627: 169–179, 1991.
- ZAR, J. H. Testing for goodness of fit. In: *Biostatistical Analysis*, edited by J. H. Zar. Englewood Cliffs, NJ: Prentice Hall, 1999, p. 461–485.
- ZUCKER, R. S. AND FOGELSON, A. L. Relationship between transmitter release and presynaptic calcium influx when calcium enters through discrete channels. *Proc. Natl. Acad. Sci. USA* 83: 3032–3036, 1986.